

AD-771 352

**ANALYSIS OF THE LINEAR PITCHING AND  
YAWING MOTION OF CURVED-FINNED MISSILES**

**Frank L. Stevens**

**Naval Weapons Laboratory  
Dahlgren, Virginia**

**October 1973**

**DISTRIBUTED BY:**

**NTIS**

**National Technical Information Service  
U. S. DEPARTMENT OF COMMERCE  
5285 Port Royal Road, Springfield Va. 22151**

UNCLASSIFIED

Security Classification

AD 771 352

## DOCUMENT CONTROL DATA - R &amp; D

(Security classification of title, body of abstract and indexing annotation must be entered when the overall report is classified)

1. ORIGINATING ACTIVITY (Corporate author)		2a. REPORT SECURITY CLASSIFICATION	
Naval Weapons Laboratory Dahlgren, Virginia 22448		UNCLASSIFIED	
3. REPORT TITLE		2b. GROUP	
ANALYSIS OF THE LINEAR PITCHING AND YAWING MOTION OF CURVED-FINNED MISSILES			
4. DESCRIPTIVE NOTES (Type of report and, inclusive dates)			
5. AUTHOR(S) (First name, middle initial, last name)			
Frank L. Stevens			
6. REPORT DATE		7a. TOTAL NO. OF PAGES	7b. NO. OF REFS
October 1973		43	
8a. CONTRACT OR GRANT NO.		9a. ORIGINATOR'S REPORT NUMBER(S)	
b. PROJECT NO.		NWL TR-2989	
c.		9b. OTHER REPORT NO(S) (Any other numbers that may be assigned this report)	
d.			
10. DISTRIBUTION STATEMENT			
Approved for Public Release; Distribution Unlimited.			
11. SUPPLEMENTARY NOTES		12. SPONSORING MILITARY ACTIVITY	
13. ABSTRACT			
<p>Maple-Synge theory is used to establish the analytical form of the aerodynamic forces and moments acting on a four-finned, curved-finned vehicle. The linearized equations of motion are solved, and the effects of the curved-finned aerodynamics on the stability of motion are investigated. It is shown that small and moderate values of yawing moment due to angle-of-attack, characteristic of curved-finned configurations, can have significant effects on both transient and steady-state stability.</p>			

Reproduced by  
NATIONAL TECHNICAL  
INFORMATION SERVICE  
U S Department of Commerce  
Springfield VA 22151

DD FORM 1473

1 NOV 65

(PAGE 1)

0102-014-6700

UNCLASSIFIED  
Security Classification

43

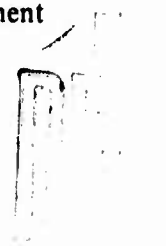
NWL Technical Report No. TR-2989  
October 1973

**ANALYSIS OF THE  
LINEAR PITCHING AND YAWING MOTION OF  
CURVED-FINNED MISSILES**

by

Frank L. Stevens

Warfare Analysis Department




Approved for Public Release; Distribution Unlimited

## **FOREWORD**

This report constitutes the first phase of a study to define the flight performance and stability characteristics of air-launched, curved-finned rockets. This work was performed under AIRTASK A3203200/009B/3F32-323-201.

This report was reviewed by Dr. T. A. Clare, Head, Flight Dynamics Group and R. D. Cuddy, Head, Aeroballistics Division.

Released by:



**RALPH A. NIEMANN**

**Head, Warfare Analysis Department**

### **ABSTRACT**

Maple-Synge theory is used to establish the analytical form of the aerodynamic forces and moments acting on a four-finned, curved-finned vehicle. The linearized equations of motion are solved, and the effects of the curved-finned aerodynamics on the stability of motion are investigated. It is shown that small and moderate values of yawing moment due to angle-of-attack, characteristic of curved-finned configurations, can have significant effects on both transient and steady-state stability.

## CONTENTS

	Page
FOREWORD . . . . .	i
ABSTRACT . . . . .	ii
I. INTRODUCTION . . . . .	1
II. ANALYSIS . . . . .	2
A. General Equations of Motion . . . . .	2
B. Solution for Linear Aerodynamics . . . . .	5
C. Effects of Curved Fins on Stability . . . . .	9
III. DISCUSSION OF RESULTS . . . . .	12
A. Transient Stability . . . . .	12
B. Steady-State Motion . . . . .	14
C. Numerical Simulation . . . . .	18
IV. CONCLUSIONS AND FUTURE PLANS . . . . .	25
REFERENCES . . . . .	26
APPENDICES	
A. List of Symbols	
B. Maple-Synge Analysis of Four-Finned, Curved-Finned Missile	
C. Distribution	

## I. INTRODUCTION

The use of curved fins as missile stabilizers has increased significantly in recent years. This is due in large part to the inherent suitability of such configurations for tube-launched ordnance (minimal volume used for fin storage). Curved-finned missiles, due to their "non-mirror symmetry" properties, can have aerodynamic characteristics considerably different from the familiar cruciform-finned configurations. This is evidenced by the "zero fin cant" roll moment produced by curved fins; this has been extensively studied<sup>1,2,3</sup> and found to be strongly dependent on Mach number and angle-of-attack, as well as on fin geometry.

The Naval Weapons Laboratory is conducting a program to define the flight performance characteristics of curved-finned vehicles for present and future flight conditions characteristic of air-launched, tactical rockets. It is the purpose of this report to document the initial phase of this effort: examination of the effects of the non-mirror symmetry of curved fins on the linear pitching and yawing motion of finned missiles. Theoretical expressions for the linear aerodynamic force and moment systems for a curved-finned body are presented, and the equations of motion with these aerodynamics are solved. The effects of the non-mirror symmetry terms on the stability of motion are investigated, and it is shown that small values of the yawing moment due to angle-of-attack can lead to reduced dynamic stability or dynamic instability. Numerical verification of these results is presented.

## II. ANALYSIS

### A. General Equations of Motion

This analysis is concerned with the transverse angular motion of rolling four-finned, curved-finned missiles. A sketch of a typical curved-finned rocket configuration is shown in Figure 1. For such a configuration, it is convenient to write the equations of motion in an aeroballistic axis system<sup>4</sup> which pitches and yaws with the body but does not roll (Figure 2). For this axis system, the equations of motion may be written as

$$\vec{F} = m\dot{\vec{V}} + \vec{\Omega}_s \times \vec{V} \quad (1)$$

$$\vec{M} = \vec{I} \cdot \dot{\vec{\Omega}}_B + \vec{\Omega}_s \times (\vec{I} \cdot \vec{\Omega}_B)$$

where

$$\vec{V} = \begin{Bmatrix} u \\ v \\ w \end{Bmatrix} \quad \vec{\Omega}_B = \begin{Bmatrix} p \\ q \\ r \end{Bmatrix} \quad \vec{\Omega}_s = \begin{Bmatrix} 0 \\ q \\ r \end{Bmatrix}$$

$$\vec{F} = \begin{Bmatrix} X + g_x \\ Y + g_y \\ Z + g_z \end{Bmatrix} \quad \vec{M} = \begin{Bmatrix} L \\ M \\ N \end{Bmatrix}$$

$$\vec{I} = \begin{bmatrix} I_x & 0 & 0 \\ 0 & I & 0 \\ 0 & 0 & I \end{bmatrix}$$

Taking the transverse components of Equations (1) and neglecting gravity gives



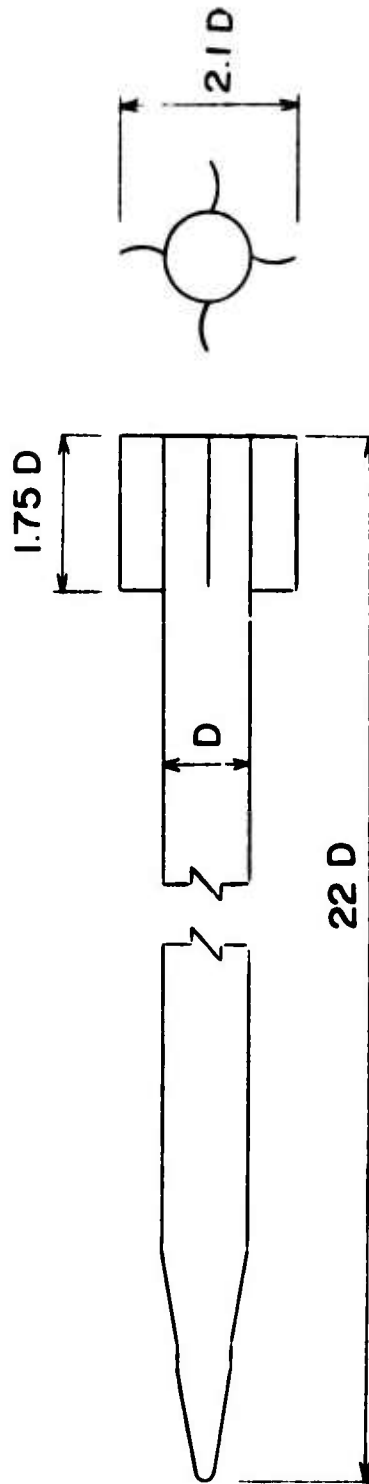
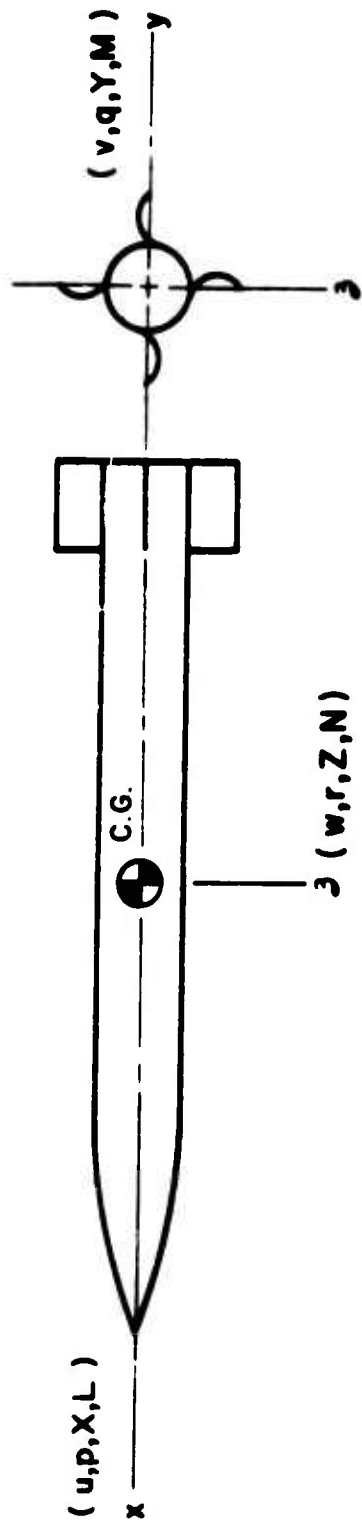


**FIGURE 1**  
Sketch of Typical Air-Launched  
Curved-Finned Rocket Configuration



$$\vec{V} = \begin{bmatrix} u \\ v \\ w \end{bmatrix}$$

$$\vec{\Omega}_B = \begin{bmatrix} p \\ q \\ r \end{bmatrix}$$

$$\vec{F} = \begin{bmatrix} X + g_x \\ Y + g_y \\ Z + g_z \end{bmatrix}$$

$$\vec{M} = \begin{bmatrix} L \\ M \\ N \end{bmatrix}$$

$$\vec{\Omega}_B = \begin{bmatrix} 0 \\ q \\ r \end{bmatrix}$$

FIGURE 2

Aeroballistic Axis System and Vector Quantities

$$\dot{v} + ur = \frac{Y}{m}$$

$$\dot{w} - uq = \frac{Z}{m}$$

$$\dot{q} + \frac{I_x}{I} pr = \frac{M}{I}$$

$$\dot{r} - \frac{I_x}{I} pq = \frac{N}{I}$$

(2)

By defining the complex quantities  $\bar{\alpha}$  and  $\bar{\omega}$  as

$$\bar{\alpha} = \frac{v + iw}{V}; \quad \bar{\omega} = q + ir$$

(3)

Equations (2) can be written as

$$\dot{\bar{\alpha}} - i\bar{\omega} = (Y + iZ)/mV$$

(4)

$$\dot{\bar{\omega}} - i\bar{P}\bar{\omega} = (M + iN)/I$$

where

$$\bar{P} = pI_x/I$$

and it is assumed that  $u \approx V$  (implying small angles of attack and sideslip).

### B. Solution for Linear Aerodynamics

Equations (4) can be solved analytically only if the aerodynamic forces and moments can be expressed as functions of the variables  $\bar{\alpha}$  and  $\bar{\omega}$ . The solutions to these equations have been extensively studied for aerodynamics typical of non-finned and cruciform-finned missiles.<sup>4,5</sup> The non-mirror symmetry of curved fins,

however, allows additional terms to be included in the aerodynamic expressions. It is primarily the effect of these terms on the solution to Equations (4) which will be investigated in this report.

Maple and Synge<sup>6</sup> have presented a method for determining the effects of body symmetry on the functional relationships between the aerodynamic forces and moments and the state of motion of the body. Appendix B presents a summary of the application of Maple-Synge theory to a four-finned, curved-finned body. The resulting linearized equations for the aerodynamics are

$$Y + iZ = (Y_0 + iZ_0)e^{ip^t} + \left[ Z_\alpha - iY_\alpha + p(Z_{p\alpha} - iY_{p\alpha}) \right] \bar{\alpha} + (Y_q - Z_q)\bar{\omega} + (Z_\dot{\alpha} + iY_\dot{\alpha})\bar{\dot{\alpha}} \quad (5)$$

$$M + iN = (M_0 + iN_0)e^{ip^t} + \left[ -iM_\alpha + N_\alpha + p(N_{p\alpha} - iM_{p\alpha}) \right] \bar{\alpha} + (M_q + iN_q)\bar{\omega} + (-iM_\dot{\alpha} + N_\dot{\alpha})\bar{\dot{\alpha}} \quad (6)$$

The  $\dot{\alpha}$  derivatives, which are not accounted for by classical Maple-Synge Theory, have been included in the above equations. In addition, constant, body-fixed forces ( $Y_0$ ,  $Z_0$ ) and moments ( $M_0$ ,  $N_0$ ) have been included to account for small asymmetries or control deflections. Table 1 presents a summary of the linearized aerodynamic derivatives for missiles with and without mirror symmetry.

Referring to Table 1, it is seen that the non-mirror symmetry of curved fins allows aerodynamic cross-coupling terms ( $N_\alpha$ ,  $N_q$ ,  $N_\dot{\alpha}$ , etc.) as well as "in-plane Magnus" derivatives ( $Z_{p\alpha}$ ,  $M_{p\alpha}$ ). The yawing moment due to angle-of-attack for curved-finned configurations,  $N_\alpha$ , is very similar to the "induced side moment"<sup>5,8</sup> for cruciform-finned missiles. The primary difference is that  $N_\alpha$  is (for linear theory) independent of roll orientation (orientation of the fins to the angle-of-attack plane), while the induced side moment is a non-linear effect highly dependent on roll orientation. As will be seen later, however, the effect of  $N_\alpha$  on the motion is similar to that due to an induced side moment at constant roll orientation.

In general, the dynamic and lag force terms in Equations (5) will have little effect on the motion. Neglecting these terms and also neglecting the asymmetry forces ( $Y_0$ ,  $Z_0$ ), Equations (4), (5), and (6) become

TABLE 1

LINEAR AERODYNAMIC DERIVATIVES FOR MISSILES WITH 90°  
ROTATIONAL SYMMETRY – WITH AND WITHOUT MIRROR SYMMETRY.

Variable	Force Derivatives		Moment Derivatives	
	Mirror Symmetry Term	Additional Term For No Mirror Symmetry	Mirror Symmetry Term	Additional Term For No Mirror Symmetry
$\alpha$ (Static Derivatives)	$Z_\alpha$	$Y_\alpha$	$M_\alpha$	$N_\alpha$
$q$ (Dynamic Derivatives)	$Z_q$	$Y_q$	$M_q$	$N_q$
$\dot{\alpha}$ (Lag Derivatives)	$Z_{\dot{\alpha}}$	$Y_{\dot{\alpha}}$	$M_{\dot{\alpha}}$	$N_{\dot{\alpha}}$
$p\alpha$ (Magnus Derivatives)	$Y_{p\alpha}$	$Z_{p\alpha}$	$N_{p\alpha}$	$M_{p\alpha}$

$$\dot{\bar{\alpha}} - i\bar{\omega} = (Z'_\alpha - iY'_\alpha)\bar{\alpha} \quad (7)$$

$$\begin{aligned} \dot{\bar{\omega}} - i\bar{p}\bar{\omega} = & (\hat{M}_0 + i\hat{N}_0)e^{ip t} + \left[ -i\hat{M}_\alpha + \hat{N}_\alpha + p(\hat{N}_{p\alpha} - i\hat{M}_{p\alpha}) \right] \bar{\alpha} \\ & + (\hat{M}_q + i\hat{N}_q)\bar{\omega} + (-i\hat{M}_\alpha + \hat{N}_\alpha)\dot{\bar{\alpha}} \end{aligned} \quad (8)$$

where

$$(\quad)' = (\quad)/mV ; \quad (\hat{\quad}) = (\quad)/l$$

Equations (7) and (8) can be combined to yield

$$\ddot{\bar{\alpha}} + (a_r + ia_i)\dot{\bar{\alpha}} + (b_r + ib_i)\bar{\alpha} = i(\hat{M}_0 + i\hat{N}_0)e^{ip t} \quad (9)$$

where

$$\begin{aligned} a_r &= -\hat{M}_q - \hat{M}_\alpha - Z'_\alpha \\ a_i &= -\hat{N}_q - \hat{N}_\alpha + Y'_\alpha - \bar{p} \\ b_r &= -\hat{M}_\alpha - p\hat{M}_{p\alpha} + \bar{p}Y'_\alpha \\ b_i &= -\hat{N}_\alpha - p\hat{N}_{p\alpha} + \bar{p}Z'_\alpha \end{aligned} \quad (10)$$

and where the force derivatives in Equation (7) were considered constant (implying constant Mach number and dynamic pressure). In addition, products of stability derivatives were neglected in Equations (10). For constant coefficients, Equation (9) can be solved directly to give

$$\bar{\alpha} = \bar{K}_1 e^{i\omega_1 t} + \bar{K}_2 e^{i\omega_2 t} + \bar{K}_3 e^{ip t} \quad (11)$$

$$\bar{K}_{1,2} = \bar{K}_{1,2,0} e^{\lambda_{1,2} t}$$

$$\bar{K}_3 = \frac{i(\hat{M}_0 + i\hat{N}_0)}{p^2 + p(a_r + ia_i) + b_r + ib_i} \quad (12)$$

$$\lambda_{1,2} + i\omega_{1,2} = \frac{1}{2} \left[ -a_r - ia_i \pm \sqrt{a_r^2 - a_i^2 - 4b_r + i(2a_r a_i - 4b_i)} \right]$$

Therefore, it is seen that the solution to the linear equations of motion for the curved-finned vehicle takes the form of the familiar tricyclic solution for cruciform fins, with the modal frequencies,  $(\omega_{1,2})$  damping rates  $(\lambda_{1,2})$  and steady state solution  $(\bar{K}_3)$  modified due to the curved-finned aerodynamic terms.

### C. Effects of Curved Fins on Stability

Equation (11), along with Equations (10) and (12), describes the transverse angular motion for a curved-finned body with arbitrary aerodynamics. Of primary interest, however, are the effects of curved-finned aerodynamics on both the stability of transient motion and the steady-state amplitude of motion due to asymmetries. In order to investigate these effects, it is advantageous to simplify several of the above equations.

The transient stability characteristics are determined by the modal frequencies and damping rates given by the last of Equations (12). This can be rewritten as

$$\lambda_{1,2} + i\omega_{1,2} = \frac{1}{2} \left[ -a_r - ia_i \pm \sqrt{E^2 + F^2} \right] \quad (13)$$

where

$$E^2 = i^2(4b_r + a_i^2 - a_r^2)$$

$$F^2 = i(2a_r a_i - 4b_i)$$

The radical in Equation (13) can be expanded in a binomial series as

$$\sqrt{E^2 + F^2} = E + \frac{F^2}{2E} - \frac{F^4}{8E^3} + \dots \quad (14)$$

Then, using Equations (10) and (14) and neglecting second and higher order terms in the stability derivatives, the frequencies and damping factors may be written as

$$\omega_{1,2} = \frac{1}{2} \left[ \bar{P} + \hat{N}_q + \hat{N}_\alpha + Y'_\alpha \pm \sqrt{\bar{P}^2 + 2\bar{P} \left( \hat{N}_q + \hat{N}_\alpha + Y'_\alpha - \frac{2I}{I_X} \hat{M}_{p\alpha} \right) - 4\hat{M}_\alpha} \right] \quad (15)$$

$$\lambda_{1,2} = \frac{1}{2} \left[ (\hat{M}_q + \hat{M}_\alpha)(1 \pm \tau) + Z'_\alpha(1 \mp \tau) \right] \pm \frac{N_{p\alpha}}{I_X} \tau \pm \frac{\hat{N}_\alpha}{\left[ \bar{P}^2 + 2\bar{P} \left( \hat{N}_q + \hat{N}_\alpha + Y'_\alpha - \frac{2I}{I_X} \hat{M}_{p\alpha} \right) - 4\hat{M}_\alpha \right]^{1/2}} \quad (16)$$

where

$$\tau = \frac{1}{\sqrt{1 - \frac{I}{s}}} \quad (17)$$

$$s = \frac{\bar{P}^2 + 2\bar{P}(\hat{N}_q + \hat{N}_\alpha - Y'_\alpha)}{4\hat{M}_\alpha + 4\bar{P} \left( \frac{I_X}{I} \hat{M}_{p\alpha} - Y'_\alpha \right)}$$

The steady-state, or trim, angle of attack is given by the second of Equations (12) and is seen to be a function of spin rate. It is convenient to write the trim angle as<sup>5</sup>

$$\bar{K}_3 = \frac{i(\hat{M}_0 + i\hat{N}_0)}{[i(p - \omega_1) - \lambda_1][i(p - \omega_2) - \lambda_2]} \quad (18)$$

The effects of spin rate on the steady-state trim angle can be investigated by introducing the trim amplification factor,  $f$ , defined as

$$f = \frac{i\bar{K}_3}{|\bar{K}_3|_{p=0}} \quad (19)$$

The zero-spin trim angle is

$$\bar{K}_{3p=0} = \frac{-i(\hat{M}_0 + i\hat{N}_0)}{\hat{M}_\alpha + i\hat{N}_\alpha}$$



Therefore, by using Equations (18) and (20), the trim amplification factor is

$$f = \left\{ \frac{\hat{M}_a^2 + \hat{N}_a^2}{[(p - \omega_1)(p - \omega_2)]^2 + (\lambda_1 \lambda_2)^2 + \lambda_1^2(p - \omega_2)^2 + \lambda_2^2(p - \omega_1)^2} \right\}^{1/2} \quad (21)$$

The transient and steady-state stability characteristics of curved-finned bodies may thus be investigated by the use of Equations (15), (16), and (21). These characteristics will be quantitatively discussed in the following section.

### III. DISCUSSION OF RESULTS

#### A. Transient Stability

The requirement for static stability is

$$\bar{p}^2 + 2\bar{p}(\hat{N}_q + \hat{N}_\alpha + Y'_\alpha - \frac{2l}{I_x} \hat{M}_{p\alpha}) - 4\hat{M}_\alpha > 0 \quad (22)$$

Equation (16) indicates the possibility of static instabilities occurring in curved-finned missiles with a negative restoring moment (e.g.,  $M_\alpha < 0$ ). The static stability requirement is shown graphically in Figure 3, where

$$\tilde{p} = \frac{\bar{p}}{-4\hat{M}_\alpha}$$

$$A = \frac{\hat{N}_q + \hat{N}_\alpha + Y'_\alpha - \frac{l}{I_x} \hat{M}_{p\alpha}}{\sqrt{-4\hat{M}_\alpha}}$$

From the figure, it is seen that gyroscopic instabilities are not possible for magnitudes of  $\tilde{p}$  or  $A$  less than 1. For most finned rockets, the static margin is large ( $M_\alpha \ll 0$ ) and  $l_x/l \ll 1$ . Thus the magnitude of  $\tilde{p}$  will usually be much less than 1. Furthermore, although the magnitudes of the curved-finned aerodynamic derivatives are not generally known at this time, it is expected that they will be small compared to the restoring moment. The magnitude of  $A$  should therefore also be much less than 1. Except for cases of small static margin, then, the curved-finned effects on the gyroscopic stability should be small.

In light of the above discussion, the curved-finned terms in the denominator of the last term of Equation (16) will be neglected, so that

$$\lambda_{1,2} = \frac{1}{2} \left[ (\hat{M}_q + \hat{M}_\alpha)(1 \pm \tau) + Z'_\alpha(1 \mp \tau) \right] \pm \frac{N_{p\alpha}\tau}{I_x} \quad (23)$$

$$\pm \frac{\hat{N}_\alpha}{|p^2 - 4\hat{M}_\alpha|^{1/2}}$$

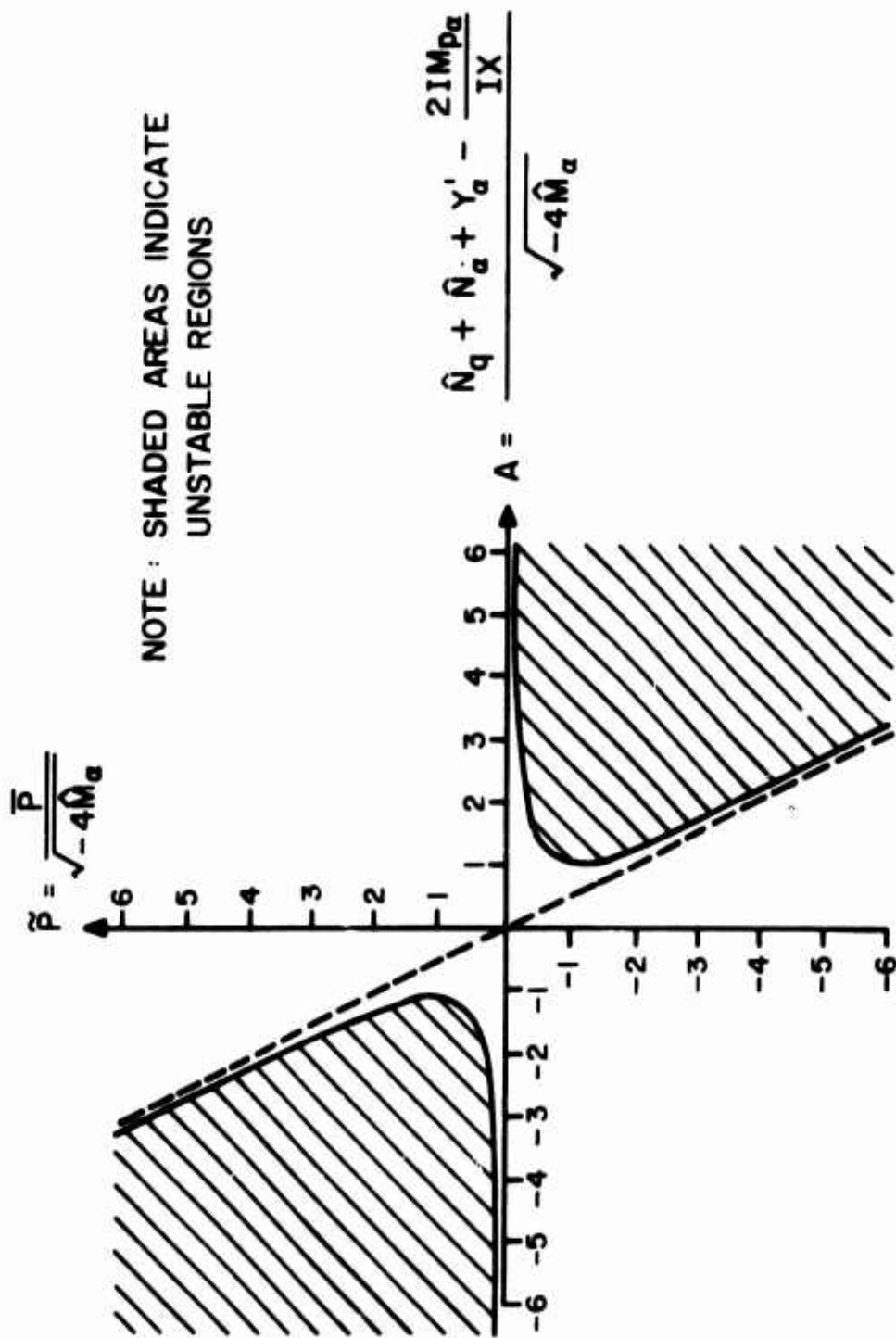


FIGURE 3

Static Stability Requirements For Curved-Finned Missiles

The requirements for dynamic stability are

$$\lambda_{1,2} < 0$$

For typical spin rates of finned bodies,  $\tau$  can be neglected with respect to 1, and the requirement for dynamic stability becomes

$$\left| \frac{\hat{N}_\alpha}{\sqrt{-4\hat{M}_\alpha + p^2}} + \frac{N_{p\alpha}\tau}{I_X} \right| < -(\hat{M}_q + \hat{M}_\alpha + Z'_d) \quad (24)$$

Using the set of parameters shown in Table 2, which are typical of air-launched rocket configurations (with  $N_{p\alpha}$  taken as zero for convenience), the magnitude of  $N_\alpha$  required to introduce dynamic instability (assuming zero spin rate) was computed and found to be approximately 8%  $M_\alpha$ . The variation of the damping factors with  $N_\alpha$  for these data are shown in Figure 4.

Spin rates up to 300 rad/sec were also investigated, but were found to have little effect on the damping factors or the magnitude of  $N_\alpha$  leading to instability. For non-zero Magnus ( $N_{p\alpha}$ ), however, the damping factors and critical magnitude of  $N_\alpha$  could vary significantly with spin rate.

## B. Steady-State Motion

The steady-state amplitude of motion is dependent on spin rate, and the familiar resonance condition for finned bodies occurs when  $p = \omega_1$ ; from Equation (21), the magnification factor at this condition is

$$f_{p=\omega_1} = \frac{1}{\lambda_1} \left[ \frac{\hat{M}_\alpha^2 + \hat{N}_\alpha^2}{\lambda_2^2 + (p - \omega_2)^2} \right]^{1/2} \quad (25)$$

Equation (25) indicates the sensitivity of the resonance magnification factor to changes in the nutation damping factor,  $\lambda_1$ . Therefore, depending on its magnitude, the term  $N_\alpha$  can lead to a significant alteration of the resonance amplification factor, as seen in Figure 5. These results were also computed using the parameters in Table 2.

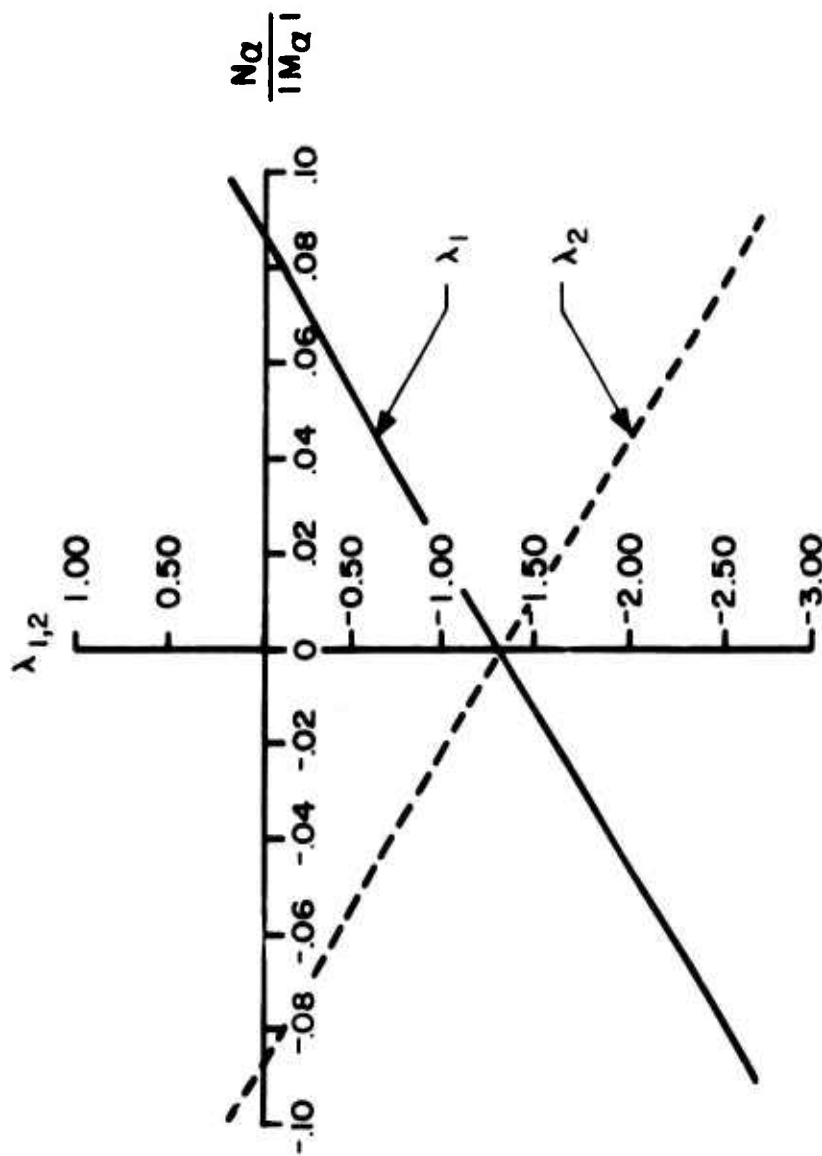


**FIGURE 4**  
**Effect of  $N_\alpha$  On Dynamic Stability**  
**(Parameters in Table 2 and  $p = 0$ )**

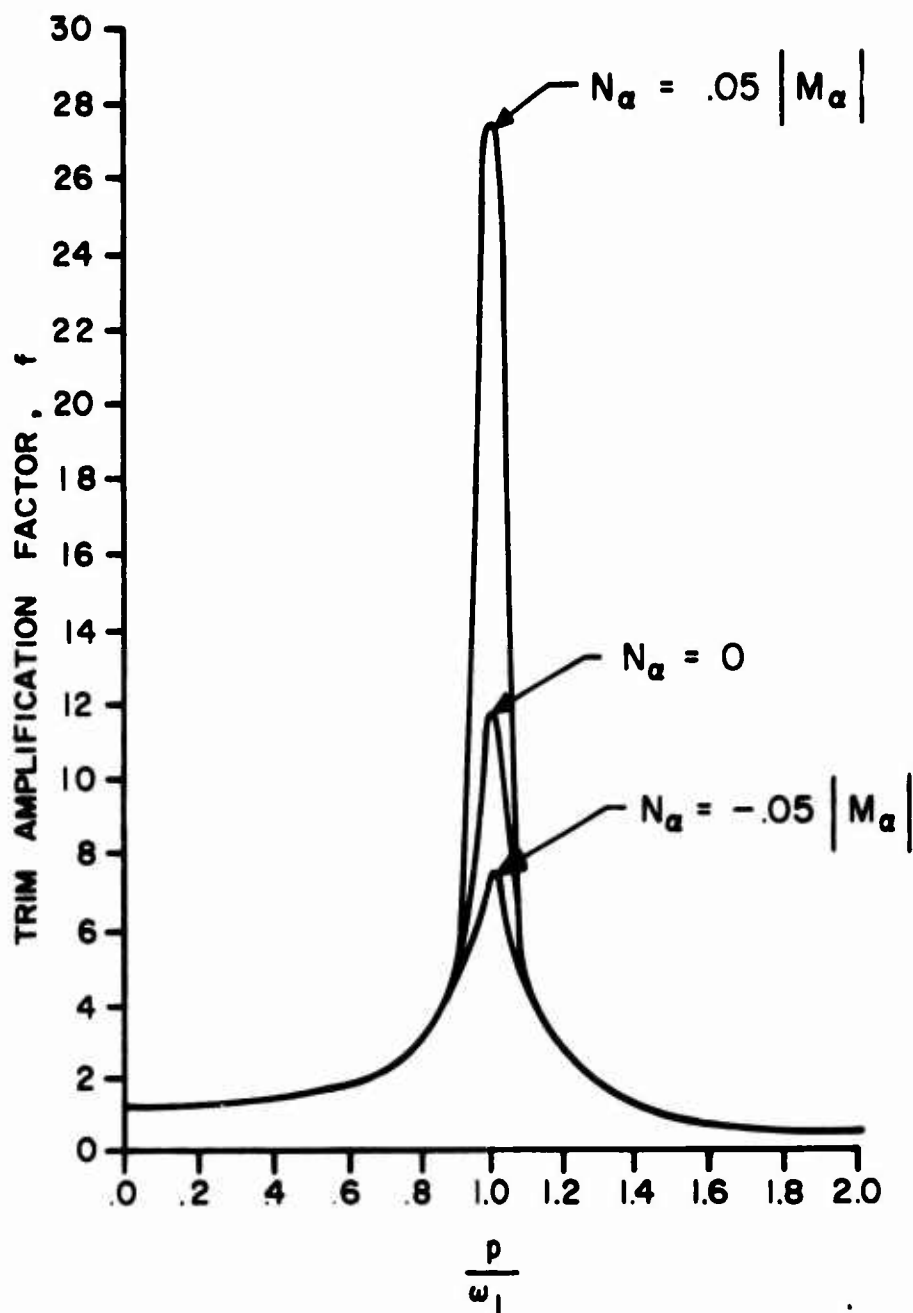


FIGURE 5

Effect of  $N_\alpha$  On Amplitude of Trim  
(Parameters in Table 2)

**TABLE 2**

**AERODYNAMIC COEFFICIENTS, MASS AND FLOW  
PARAMETERS USED FOR NUMERICAL SIMULATIONS**

$$C_{M\alpha} = -68.32 \text{ rad}^{-1}$$

$$C_{Z\alpha} = -9.19 \text{ rad}^{-1}$$

$$d = .4167 \text{ ft}$$

$$I_x = .07 \text{ sl} \cdot \text{ft}^2$$

$$\rho = .001756 \text{ sl/ft}^3$$

$$m = 2.92 \text{ slugs}$$

$$C_{Mq} + C_{M\alpha} = -1500.0 \text{ rad}^{-1}$$

$$C_{Np\alpha} = 0$$

$$S = .13635 \text{ ft}^2$$

$$I = 23.01 \text{ sl} \cdot \text{ft}^2$$

$$V = 2500 \text{ ft/sec}$$

### C. Numerical Simulation

Equations (2) were numerically integrated using the parameters in Table 2 and compared to results using Equation (11) for several combinations of spin rate and  $N_\alpha$ . In all cases, excellent agreement between the two solutions was obtained; Figure 6 shows the comparison for one set of conditions which gave a precession instability. Equations (15) and (16) were found to give good results for the modal frequencies and damping factors, respectively.

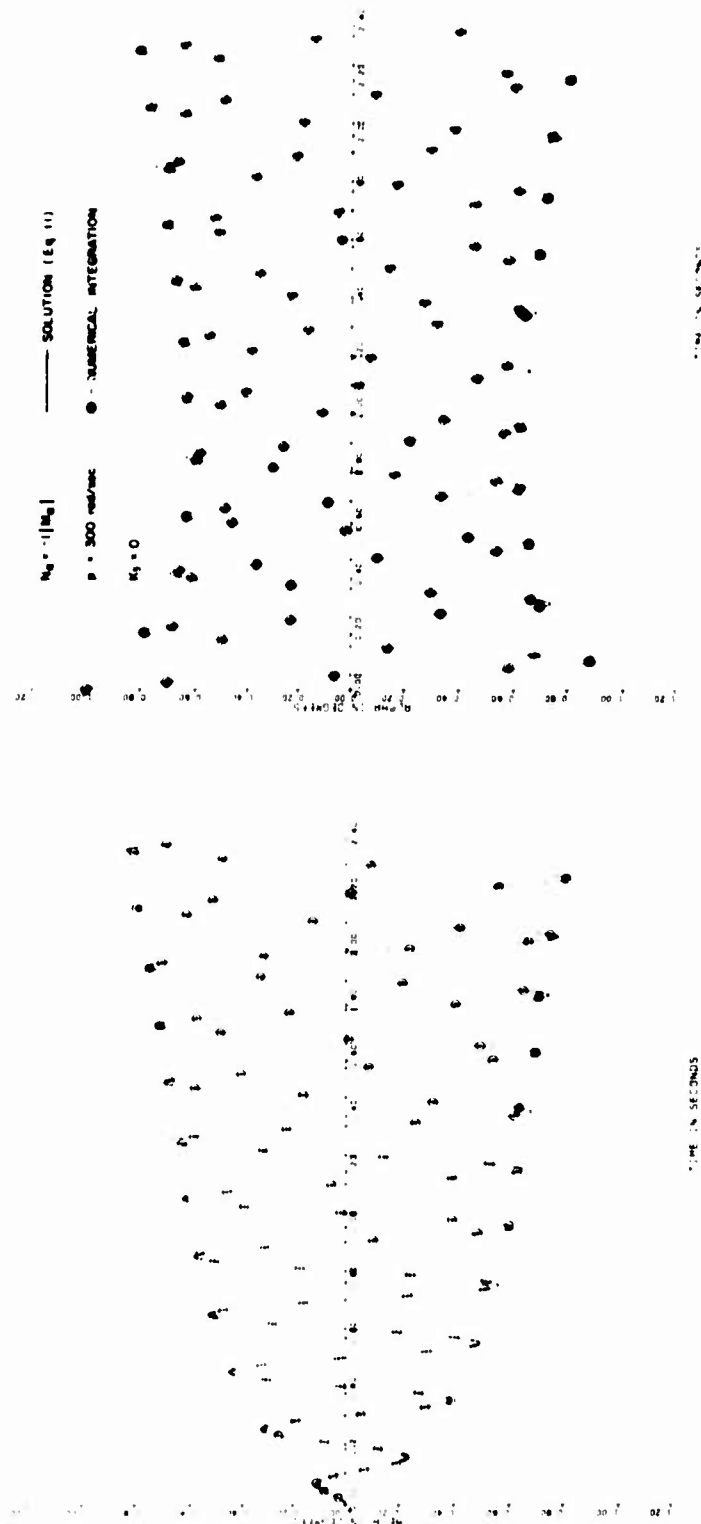
Equation (24) indicated that  $|N_\alpha/M_\alpha| < .08$  was necessary for stability for the parameters in Table 2 and zero spin rate. Figure 7 shows a precession instability for  $N_\alpha/|M_\alpha| = -.10$ . For  $N_\alpha = -.05|M_\alpha|$ , the motion is dynamically stable (Figure 8).

Figure 4 shows that any non-zero value of  $N_\alpha$  causes unequal damping rates ( $\lambda$ 's) of the nutation and precession arms. This gives rise to the circular motion illustrated in Figures 7 and 8 for both stable and unstable cases, respectively. As mentioned earlier, this type of motion is also characteristic of cruciform-finned missiles at constant roll orientation (implying roll rate equal to the coning frequency) when acted on by an induced side moment.

The instability associated with an induced side moment – commonly known as "Catastrophic Yaw" – can occur only for sustained spin rates at or near the nutation frequency. As shown earlier, however, sufficient magnitudes of  $N_\alpha$  can lead to instabilities for curved-finned configurations at zero roll rate. It is interesting to note that a similar type of instability – circular motion with near zero spin – was observed in flights of tangent-finned rockets,<sup>9</sup> which have the same symmetry properties as curved-finned vehicles. This instability was postulated to have been caused by a non-linear damping moment. The static side moment derivative,  $N_\alpha$  discussed in this report (or its higher order non-linearities) is an alternate explanation for these observed motions.

Figures 9, 10, and 11 show the complex motion at resonance for a zero spin trim amplitude of  $1^\circ$  and values of  $N_\alpha$  of 0 and  $\pm 5\% M_\alpha$ , respectively. The amplitude of the steady-state motion is seen to agree well with that predicted by Equation (21) and shown in Figure 5.





**FIGURE 6**  
**Comparison of Solution With Numerical Integration**

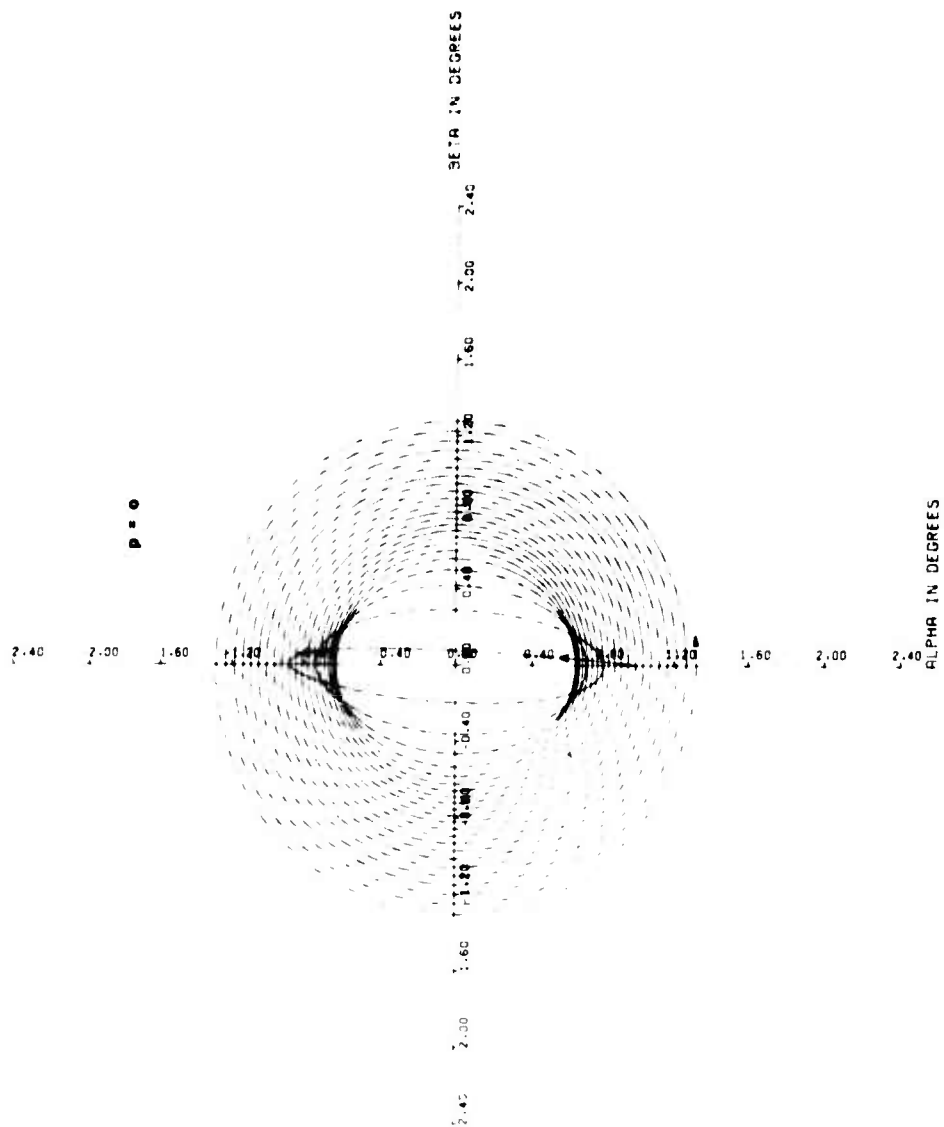


**FIGURE 7**

**Complex Angular Motion ( $N_\alpha = -.1 M |M_\alpha|$ )**

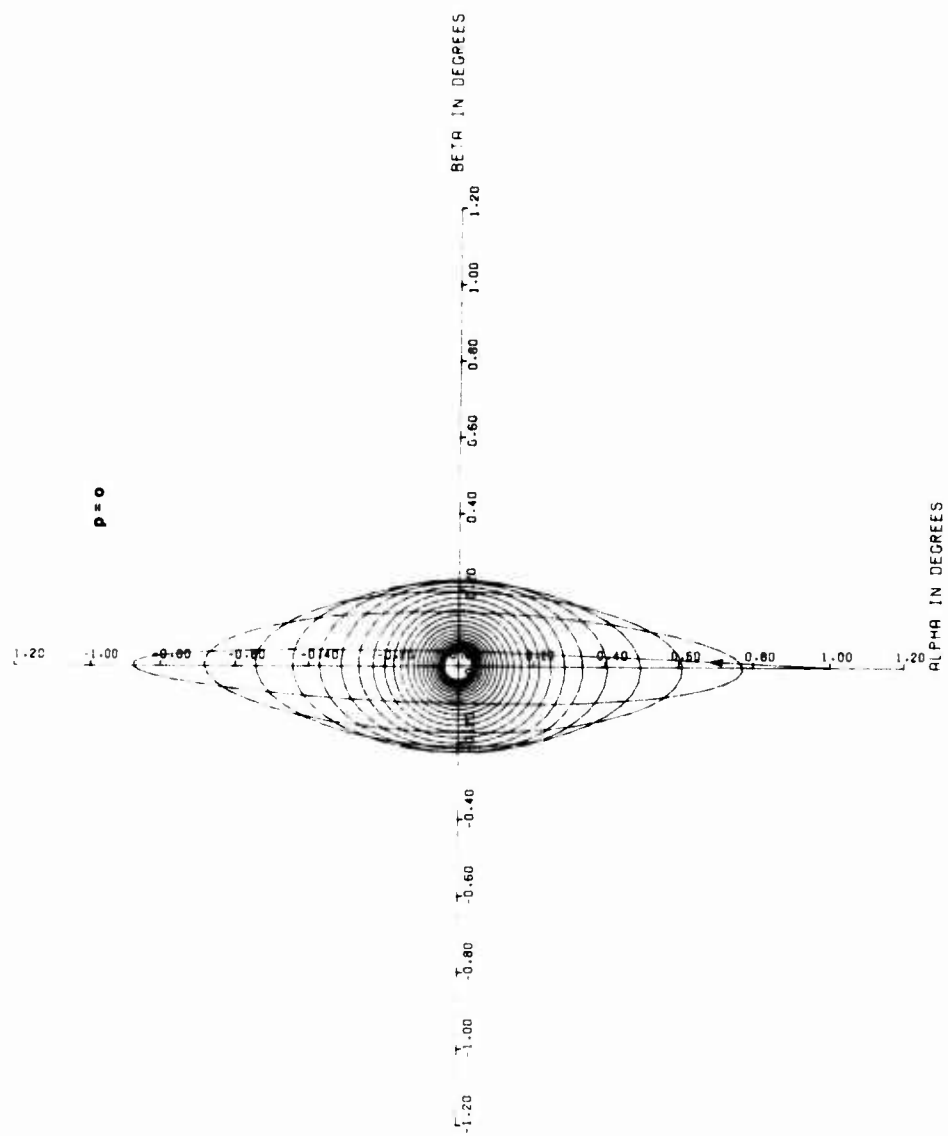


**FIGURE 8**

**Complex Angular Motion ( $N_\alpha = -.05 |M_\alpha|$ )**

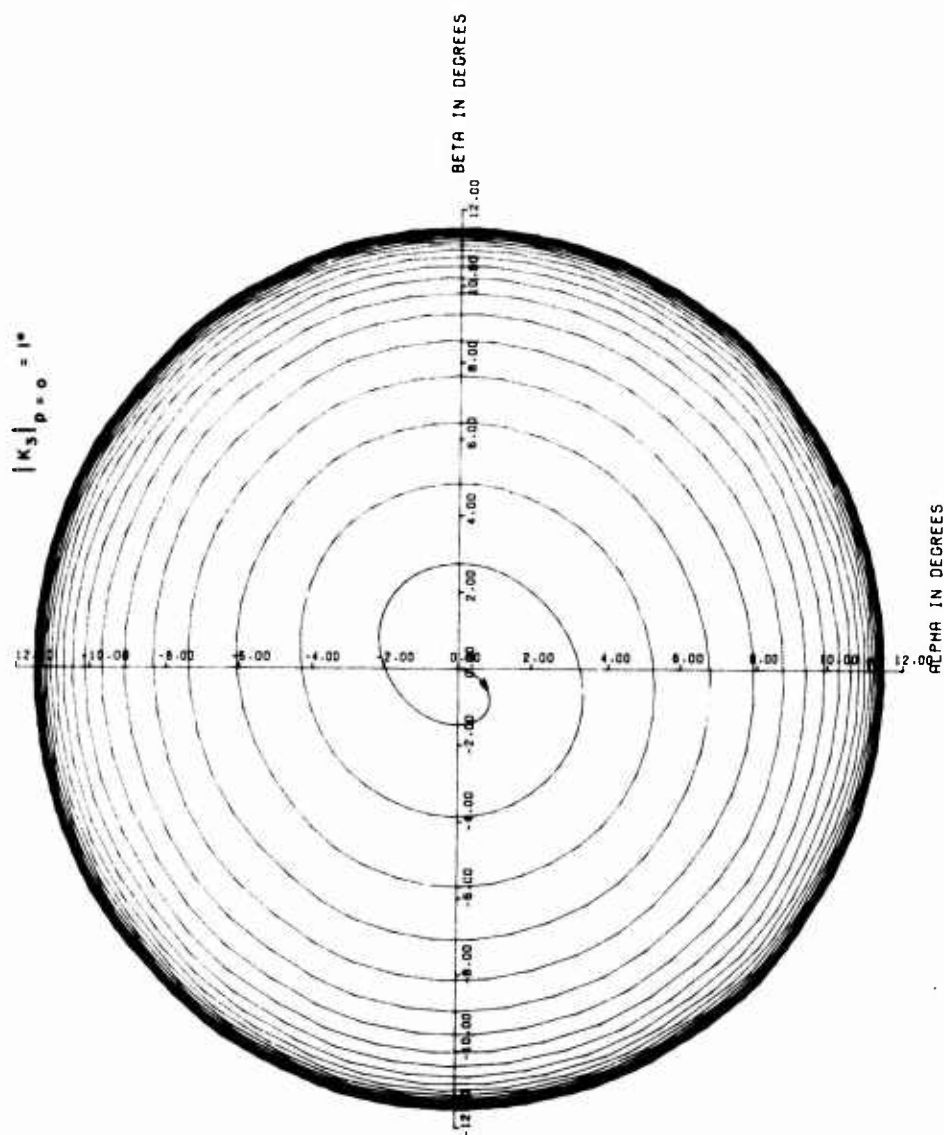


**FIGURE 9**

**Complex Angular Motion At Resonance ( $N_\alpha = 0$ )**

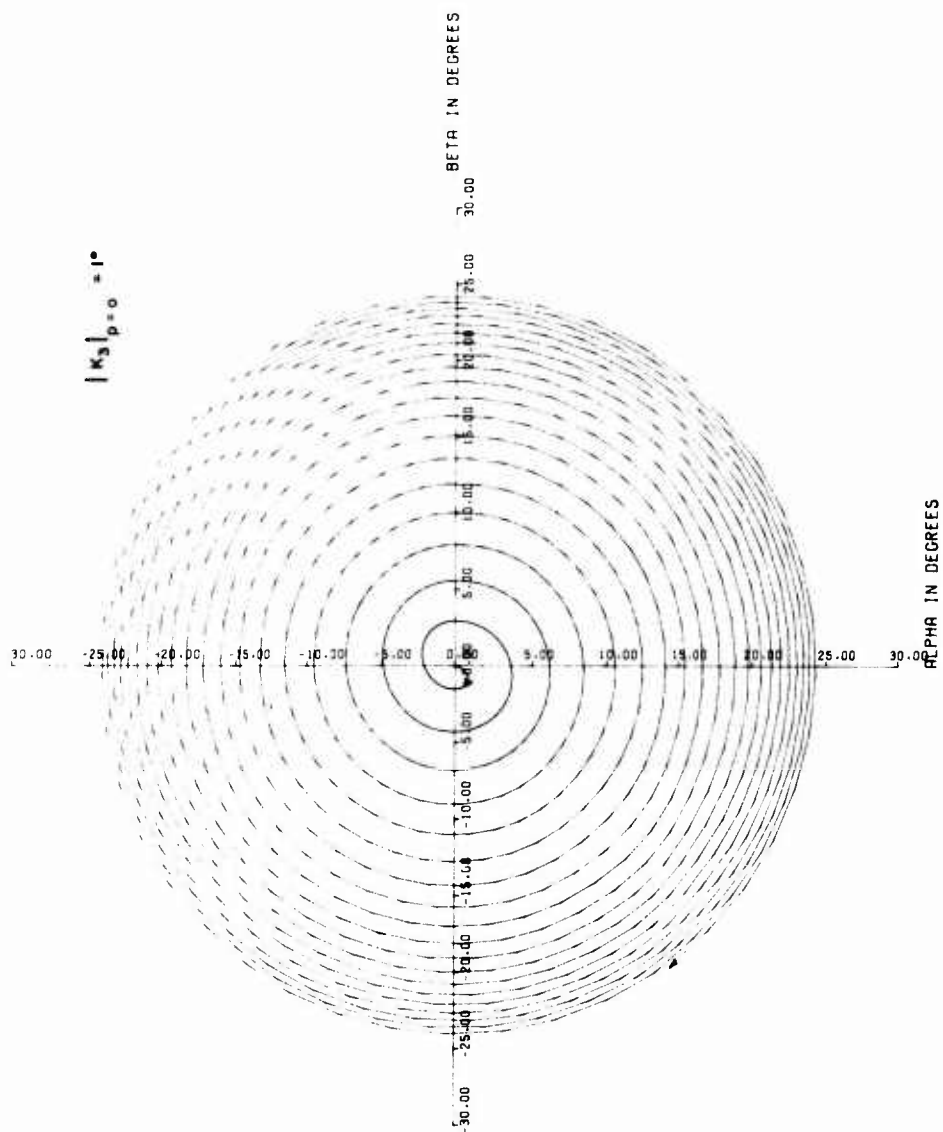


**FIGURE 10**

**Complex Angular Motion At Resonance ( $N_\alpha = .05 |M_\alpha|$ )**

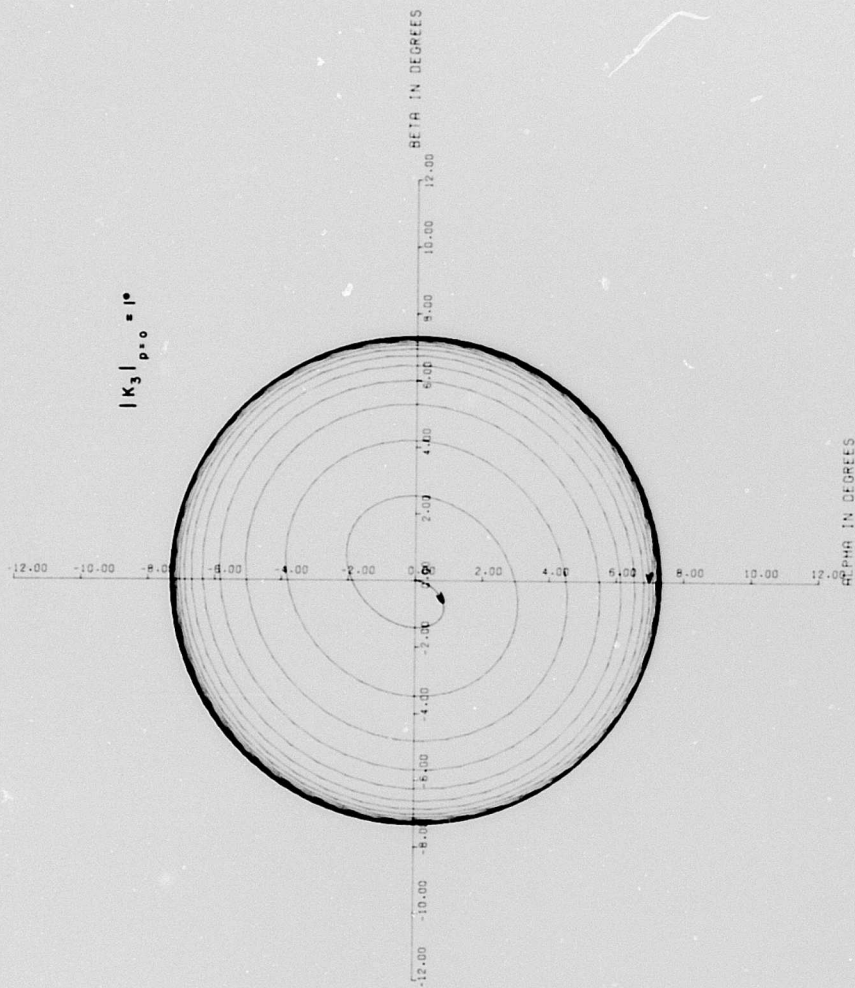


FIGURE 11

Complex Angular Motion At Resonance ( $N_\alpha = - .05 |M_\alpha|$ )

#### IV. CONCLUSIONS AND FUTURE PLANS

Maple-Syngé theory was used to determine the analytical form of the aerodynamic forces and moments acting on a four-finned, curved-finned missile. The resulting linear equations of motion were solved for constant spin rate and aerodynamics, and stability criteria were derived. The analysis showed that:

- 1) Except for cases of small static margin, the modal frequencies are relatively insensitive to aerodynamics peculiar to curved fins and can be considered the same as for cruciform-finned missiles.
- 2) The modal damping factors can be seriously affected by the side moment derivative,  $N_{\alpha}$ . It was shown that, for zero Magnus moments, small values of this parameter can lead to dynamic instabilities. When Magnus contributions are considered, both the magnitude and sign of  $N_{\alpha}$  are important to the dynamic stability characteristics.
- 3) The magnitude of the trim amplification factor at spin rates near resonance is dependent on both magnitude and sign of  $N_{\alpha}$ .

Numerical simulations verified these results.

The analysis presented herein will be extended to include the effects of variable spin rate and aerodynamic non-linearities on the motion of curved-finned missiles, particularly those associated with the roll characteristics of curved fins. In addition, six-degree-of-freedom calculations will be performed on typical rocket shapes to ascertain the effects of curved-finned aerodynamics coupled with variable spin rate over trajectories typical of present and future Navy tactical applications.

## REFERENCES

1. Featherstone, H. A., *The Aerodynamic Characteristics of Curved Tail Fins*, Convair-Pomona, Report No. ERR-PO-019, September 1960.
2. Holmes, John E., *Wrap-Around Fin (WAF) Aerodynamics*, Paper No. 4, Presented at the 9<sup>th</sup> Navy Symposium on Aeroballistics, 9-11 May 1972, Johns Hopkins University, Applied Physics Laboratory, Silver Spring, Md.
3. Dunkin, O. L., *Influence of Curved-Fin Stabilizers on the Rolling-Moment Characteristics of 10-Cal. Missiles at Mach Numbers From 0.2 to 1.3*, AEDC-TR-71-237, Arnold Engineering Development Center, Arnold Air Force Station, Tennessee, October 1971.
4. Murphy, C. H., *Free-Flight Motion of Symmetric Missiles*, BRL Rpt. 1216, Ballistic Research Laboratories, Aberdeen Proving Ground, Md., 1963, AD-442757.
5. Nicolaides, John D., *Missile Flight and Astrodynamics*, Bureau of Weapons TN 100-A, 1961.
6. Maple, C. G. and Synge, J. L., "Aerodynamic Symmetry of Projectiles," *Quarterly of Applied Mathematics*, Vol. VI, No. 4, January 1949.
7. Murphy, C. H., *Effect of Symmetry on the Linearized Force System*, Technical Note No. 743, Ballistic Research Laboratories, Aberdeen Proving Ground, Md., September 1952.
8. Nicolaides, John D. and Clare, Thomas A., *Non-Linear Resonance Instability in the Flight Dynamics of Missiles*, AIAA Paper No. 70-969, AIAA Guidance, Control, and Flight Mechanics Conference, Santa Barbara, California, August 17-19 1970.
9. Stirton, R. J., *The Yawing Motion of Tangent-Finned Rockets*, NOTS Report 1867, U. S. Naval Ordnance Test Station, China Lake, California, 21 October 1957.



### **List of Symbols**

$d$	Reference Length
$\vec{F}$	External Force
$g$	Gravitational Acceleration
$I$	Transverse Moment of Inertia
$I_x$	Axial Moment of Inertia
$K$	Amplitude of Angular Motion
$L$	Moment component along x
$M$	Moment component along y
$m$	Mass
$\vec{M}$	External Moment about C. G.
$N$	Moment Component along z
$p$	Angular velocity component along x
$Q$	Dynamic pressure = $\frac{1}{2}\rho V^2$
$q$	Angular velocity component along y
$r$	Angular velocity component along z
$S$	Reference Area
$u$	Velocity component along x
$v$	Velocity component along y
$\vec{V}$	Velocity of C. G.
$w$	Velocity component along z

### List of Symbols (Continued)

<b>X</b>	Aerodynamic force component along x
<b>x</b>	Longitudinal body axis
<b>Y</b>	Aerodynamic force component along y
<b>y</b>	Transverse body (aeroballistic) axis
<b>Z</b>	Aerodynamic force component along z
<b>z</b>	Transverse body (aeroballistic) axis
$\alpha$	Angle of attack $\equiv \frac{w}{V}$
$\beta$	Angle of Sideslip $\equiv \frac{v}{V}$
$\lambda$	Angular motion damping factor
$\rho$	Atmospheric Density
$\omega$	Frequency of Angular Motion
$\tilde{\Omega}$	Angular Velocity about C. G.

#### Subscripts

$( )_B$	Body
$( )_S$	Axis System
$( )_x$	Component along x
$( )_y$	Component along y
$( )_z$	Component along z
$( )_0$	Initial or constant value
$( )_1$	Nutation arm of tricyclic motion
$( )_2$	Precession arm of tricyclic motion
$( )_3$	Trim arm of tricyclic motion

### Superscripts

$\overline{(\ )}$	Complex Quantity
$\vec{(\ )}$	Vector Quantity
$\overset{\leftrightarrow}{(\ )}$	Tensor Quantity
$\dot{(\ )}$	$d(\ )/dt$

### Aerodynamic Derivatives

$$M_{\alpha} = QSdC_{M_{\alpha}} = \text{Static Moment Derivative}$$

$$M_q = \frac{QSd^2}{2V} C_{M_q} = \text{Damping Moment Derivative}$$

$$M_{\dot{\alpha}} = \frac{QSd^2}{2V} C_{M_{\dot{\alpha}}} = \text{Lag Moment Derivative}$$

$$^*M_{p\alpha} = \frac{QSd^2}{2V} C_{M_{p\alpha}} = \text{"In-Plane Magnus" Moment Derivative}$$

$$^*N_{\alpha} = QSdC_{N_{\alpha}} = \text{Static Side Moment Derivative}$$

$$^*N_q = \frac{QSd^2}{2V} C_{N_q} = \text{Dynamic Side Moment Derivative}$$

$$^*N_{\dot{\alpha}} = \frac{QSd^2}{2V} C_{N_{\dot{\alpha}}} = \text{Lag Side Moment Derivative}$$

$$N_{p\alpha} = \frac{QSd^2}{2V} C_{N_{p\alpha}} = \text{Magnus Moment Derivative}$$

$$^*Y_{\alpha} = QSC_{Y_{\alpha}} = \text{Static Side Force Derivative}$$

$$^*Y_q = \frac{QSd}{2V} C_{Y_q} = \text{Dynamic Side Force Derivative}$$

$$^*Y_{\dot{\alpha}} = \frac{QSd}{2V} C_{Y_{\dot{\alpha}}} = \text{Lag Side Force Derivative}$$

$$Y_{p\alpha} = \frac{QSd}{2V} C_{Y_{p\alpha}} = \text{Magnus Force Derivative}$$

$$Z_q = QSC_{Z_q} = \text{Normal Force Derivative}$$

$$Z_{\dot{q}} = \frac{QSd}{2V} C_{Z_{\dot{q}}} = \text{Damping Force Derivative}$$

\*Indicates Terms Peculiar to Curved Fins

### **Aerodynamic Derivatives (Continued)**

$$Z_{\dot{\alpha}} = \frac{QSd}{2V} C_{Z_{\dot{\alpha}}} = \text{Lag Force Derivative}$$

$$^*Z_{p\alpha} = \frac{QSd}{2V} C_{Z_{p\alpha}} = \text{"In-Plane Magnus" Force Derivative}$$

**\*Indicates Terms Peculiar to Curved Fins**

## Maple-Synge Analysis of Four-Finned, Curved-Finned Missile

The basic assumption of Maple-Synge theory is that, for constant fluid properties, the aerodynamic forces and moments can be expressed as Taylor Series expansions in the instantaneous linear and angular velocity components of the body. Under this assumption, then, the effects of the body's symmetry characteristics on these expansions can be ascertained.

By virtue of this assumption, the aerodynamic force and moment components along body-fixed axes (see Figure B-1) may be written as

$$\begin{aligned}
 X &= \sum X_{abcdef} u^a v^b w^c p^d q^e r^f \\
 Y &= \sum Y_{abcdef} u^a v^b w^c p^d q^e r^f \\
 Z &= \sum Z_{abcdef} u^a v^b w^c p^d q^e r^f \\
 L &= \sum L_{abcdef} u^a v^b w^c p^d q^e r^f \\
 M &= \sum M_{abcdef} u^a v^b w^c p^d q^e r^f \\
 N &= \sum N_{abcdef} u^a v^b w^c p^d q^e r^f
 \end{aligned}
 \tag{B-1}$$

where

$$\Sigma \equiv \sum_{abcdef}$$

Consider now a new set of body axes,  $x'y'z'$ , obtained by a  $90^\circ$  rotation about  $x$  (Figure B-2). For this set of axes, the aerodynamic forces and moments are

NOTE:

$x(u,p,X,L)$  IS  
POSITIVE INTO  
PAPER

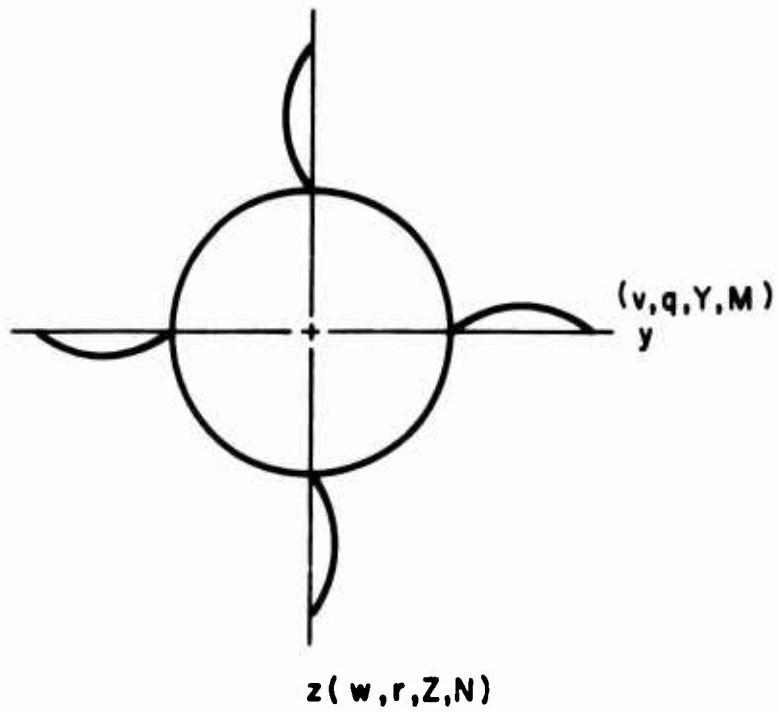


FIGURE B-1

Axis System and Vector Components  
For Maple – Synge Analysis

NOTE :

$x'(u', p', X', L')$  IS  
POSITIVE INTO  
PAPER

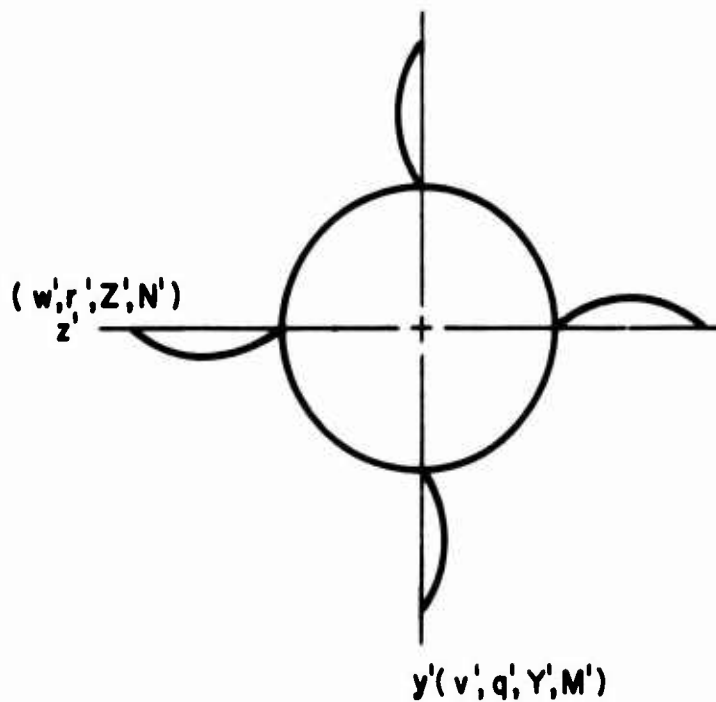


FIGURE B-2

Rotated Axis System and Vector Components  
For Maple - Synge Analysis



$$\begin{aligned}
X' &= \Sigma X'_{abcdef} u'^a v'^b w'^c p'^d q'^e r'^f \\
Y' &= \Sigma Y'_{abcdef} u'^a v'^b w'^c p'^d q'^e r'^f \\
Z' &= \Sigma Z'_{abcdef} u'^a v'^b w'^c p'^d q'^e r'^f \\
L' &= \Sigma L'_{abcdef} u'^a v'^b w'^c p'^d q'^e r'^f \\
M' &= \Sigma M'_{abcdef} u'^a v'^b w'^c p'^d q'^e r'^f \\
N' &= \Sigma N'_{abcdef} u'^a v'^b w'^c p'^d q'^e r'^f
\end{aligned}
\tag{B-2}$$

Since the body possesses 4-fold rotational symmetry, the body remains unchanged with respect to the two axis systems. Therefore, since the coefficients in the Taylor series expansions are functions only of the body geometry, they must be the same for the two systems. Or

$$\begin{aligned}
X'_{abcdef} &= X_{abcdef} \\
&\vdots \\
N'_{abcdef} &= N_{abcdef}
\end{aligned}
\tag{B-3}$$

If the same state of motion is considered, the force and moment system must be the same for the two axis systems, and

$$\begin{aligned}
u' &= u & v' &= w & w' &= -v \\
p' &= p & q' &= r & r' &= -q
\end{aligned}
\tag{B-4}$$

$$\begin{aligned}
X' &= X & Y' &= Z & Z' &= -Y \\
L' &= L & M' &= N & N' &= -M
\end{aligned}
\tag{B-5}$$

By use of Equations (B-3), (B-4), and (B-5), Equations (B-1) and (B-2) can be combined:

$$\begin{aligned}
\Sigma X_{abcdef} u^a v^b w^c p^d q^e r^f &= \Sigma (-1)^{c+f} X_{abcdef} u^a w^b v^c p^d q^e r^f \\
\Sigma Y_{abcdef} u^a v^b w^c p^d q^e r^f &= \Sigma (-1)^{c+f+1} Z_{abcdef} u^a w^b v^c p^d q^f r^e \\
\Sigma Z_{abcdef} u^a v^b w^c p^d q^e r^f &= \Sigma (-1)^{c+f} Y_{abcdef} u^a w^b v^c p^d q^f r^e
\end{aligned}
\tag{B-6}$$

$$\begin{aligned}
\Sigma L_{abcdef} u^a v^b w^c p^d q^e r^f &= \Sigma (-1)^{c+f} L_{abcdef} u^a w^b v^c p^d q^f r^e \\
\Sigma M_{abcdef} u^a v^b w^c p^d q^e r^f &= \Sigma (-1)^{c+f+1} N_{abcdef} u^a w^b v^c p^d q^f r^e \\
\Sigma N_{abcdef} u^a v^b w^c p^d q^e r^f &= \Sigma (-1)^{c+f} M_{abcdef} u^a w^b v^c p^d q^f r^e
\end{aligned}$$

The second and third of the above equations can be rewritten as

$$\begin{aligned}
\Sigma Y_{abcdef} u^a v^b w^c p^d q^e r^f &= \Sigma (-1)^{b+e+1} Z_{acbdfe} u^a v^b w^c p^d q^e r^f \\
\Sigma Z_{acbdfe} u^a w^b v^c p^d q^f r^e &= \Sigma (-1)^{c+f} Y_{abcdef} u^a w^b v^c p^d q^f r^e
\end{aligned}$$

Since the exponents are the same on both sides of these equations, each term in the summations must be equal. Therefore,

$$Y_{abcdef} = (-1)^{b+e+1} Z_{acbdfe} \tag{B-7}$$

$$Z_{acbdfe} = (-1)^{c+f} Y_{abcdef}$$

and the above equations can be satisfied for non-zero coefficients only if

$$b + c + e + f = 2n + 1 \quad (n = 0, 1, 2, \dots) \tag{B-8}$$

Therefore, the 4-fold rotational symmetry of the body requires that the force coefficients along the two transverse axes be related by Equation (B-7) and that the

exponents of the expansions satisfy Equation (B-8). When the same procedure is applied to the last two of Equations (B-6), a similar result is obtained for the transverse moments. For a 4-fold rotationally symmetric body, then

$$Y_{abcdef} = (-1)^{b+e+1} Z_{acbd ef}$$

$$N_{abcdef} = (-1)^{c+f} M_{ab cdef} \quad (B-9)$$

$$Z_{abcdef} = M_{ab cdef} = 0 \text{ for } b+c+e+f = 2n \quad (n = 0,1,2,\dots)$$

Since curved finned missiles possess no other symmetry characteristics (viz. mirror symmetry), Equations (B-9) contain all restrictions to the aerodynamics due to body symmetry. Using these equations the linear force and moment expansions can be written as

$$\begin{aligned} Y + iZ &= [Z_\alpha - iY_\alpha + p(Z_{p\alpha} - iY_{p\alpha})] \bar{\alpha} + (Y_q + iZ_q) \bar{\omega} \\ M + iN &= [-iM_\alpha + N_\alpha + p(N_{p\alpha} - iM_{p\alpha})] \alpha + (M_q + iN_q) \bar{\omega} \end{aligned} \quad (B-10)$$